Korean J. Chem. Eng., 39(12), 3412-3421 (2022)
DOI: 10.1007/s11814-022-1291-0

pISSN: 0256-1115
eISSN: 1975-7220

Phase equilibria and thermodynamic properties in the *o*-dichlorobenzene - *m*-dichlorobenzene system

Konstantin Samukov*,†, Aleksey Maksimov*, Ekaterina Belova*, Mikhail Bubenchikov, and Irina Uspenskaya***

*Chemistry Department, Lomonosov Moscow State University, 119991 Moscow, Russian Federation
**PJSC Gazprom ("TransGasTomsk"), 634029 Tomsk, Russian Federation
(*Received 18 October 2021 • Revised 19 August 2022 • Accepted 14 September 2022*)

Abstract−Rankine cycle is widely used in industry to convert heat to work using a working fluid. A mixture of *o*- and *m*-isomers of dichlorobenzene can act efficiently as a working fluid in the cycle. An equation of state (EoS) approach was chosen to model vapor-liquid equilibria and phase properties in the system. The best results were achieved with Tsai-Chen EoS. Experimental measurements of volumetric properties of mixtures and solid-liquid equilibria were performed. These data were correctly predicted within the ideal assumption. An enthalpy-pressure diagram for the *o*-dichlorobenzene - *m*-dichlorobenzene system was calculated using the resulting EoS.

Keywords: Rankine Cycle, *o*- and *m*-Dichlorobenzenes, Equation of State, Phase Equilibria, Enthalpy-pressure Diagram

INTRODUCTION

Economical usage of energy resources has become a serious problem, because oil and gas fields are exhausted and their production becomes more expensive. Waste heat not only reduces energy efficiency of a process, but also contributes to global warming. It is released in many processes and usually is absorbed by the environment. To improve energy efficiency, released heat should be taken away with a heat exchanger. Then, the heat can be used to produce work and generate electricity (for example, in the Rankine, Brighton or Stirling cycle) [1,2]. Rankine cycle is one of the most effective, cheapest and simplest thermodynamic cycles with a real working fluid [3-6].

Currently, most plants with the Rankine cycle use water as a working fluid. Organic liquids can be an alternative to water. The cycle using them is called the organic Rankine cycle (ORC) [3-8]. The reason for the choice of ORC is to make electricity generation more efficient or economically attractive for organic fluids [3-8]. Of course, the main trend at present is the development of "natural-like technologies" and "green reagents". However, sometimes situations arise where it is advisable to use toxic reagents with the necessary precautions if it is not possible to dispose of them promptly. The mixtures of *o*- and *m*-dichlorobenzenes (*o*-DCB and *m*-DCB respectively) is this case; if the removal of toxic waste is not possible all year round, it makes sense to try to use these mixtures as the working fluid of the Rankine cycle in autonomous power plants for a limited period of time, followed by disposal.

This system has not been studied enough before. To correctly design the process, it is necessary to have data on phase equilibria and phase properties. The working fluid evaporates and condensates during the Rankine cycle; therefore. it is convenient to use the equation of state (EoS) capable of describing properties of both liquid and vapor phases.

The goal of this work was to obtain parameters of an EoS for *o*-dichlorobenzene - *m*-dichlorobenzene mixtures to describe correctly thermodynamic properties of the system in a wide range of temperature and pressure. Determination of EoS parameters makes it possible to calculate an *h-P* diagram for a mixture. The diagram contains information on properties of the investigated system needed by engineers to optimize a technological scheme of the process.

EXPERIMENTAL SECTION

1. Reagents

Chemicals *o*-dichlorobenzene and *m*-dichlorobenzene were supplied by Sigma Aldrich with a stated purity ≥99%. The real purity of the compounds was determined by GC-MS analysis. The purity of *m*-dichlorobenzene was quite different from the claimed one. According to GC-MS, the main fraction of impurities in *m*-dichlorobenzene is *o*-dichlorobenzene, mixtures of two reagents can be considered as two-component systems, and so additional purification of *m*-dichlorobenzene was not carried out. The information about used reagents is listed in Table 1.

2. Methods

Densities of *o*-DCB - *m*-DCB solutions were determined with a VIP-2MP vibrating-tube densimeter. The following expression was used to obtain densities of the solutions:

$$\rho = A^* \tau^2 + B^*, \quad (1)$$

where τ is the oscillation period, A^*, B^* - coefficients, determined from calibration at the temperature measurements (288.15, 298.15, 308.15, 318.15 K) by known densities and oscillation periods of ambient air, ultrapure water and standard materials. Standard materials (Produced and certified by D.I. Mendeleyev Institute for Metrol-

†To whom correspondence should be addressed.
E-mail: samukovv@mail.ru

Table 1. Sources and purity of the chemicals

Name	CAS number	Source	Mass fraction of the main components, %	Purification/Analysis method
o-DCB	95-50-1	Sigma Aldrich	99.944	GC-MS
m-DCB	541-73-1	Sigma Aldrich	97.595	GC-MS
o-xylene	95-47-6	Component-Reaktiv	99.8	-
		DSC standards		
Hg	7439-97-6	NETZSCH	99.999	as stated by the supplier
H_2O	7732-18-5			
Ga	7440-55-3	Sigma Aldrich	99.999	as stated by the supplier
C_6H_5COOH	65-85-0	Mendeleev Research Institute for Metrology (St.-Petersburg)	99.995	as stated by the supplier
In	7440-74-6	NETZSCH	99.999	as stated by the supplier
Sn	7440-31-5	NETZSCH	99.999	as stated by the supplier
Bi	7440-69-9	NETZSCH	99.999	as stated by the supplier
Pb	7439-92-1	NETZSCH	99.999	as stated by the supplier
Zn	7440-66-6	NETZSCH	99.999	as stated by the supplier
CsCl	7647-17-8	NETZSCH	99.999	as stated by the supplier

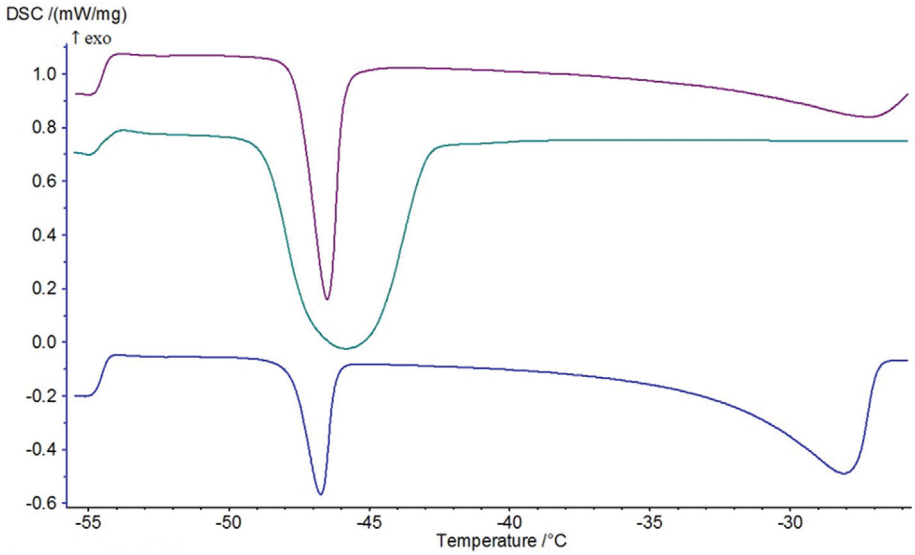

Fig. 1. DSC curves of the *o*-DCB - *m*-DCB system with *m*-DCB content (in mass fraction): 20.25 wt% (violet line), 50.02 wt% (green line) and 90.03 wt% (blue line); HR=2 K/min.

ogy VNIIM, Russia St. Petersburg) were used for 298.15 K, *o*-xylene was used for other temperatures. Temperature was maintained by a built-in thermostat, with a precision of temperature registration ±0.005 K. Standard uncertainty of a registered temperature u(T) was 0.02 K. Standard deviation for measurement of one solution was 0.0001 g/ml. Atmosphere pressure was recorded during all the experiments. Standard uncertainty of registered pressure u(P) was 1 kPa.

DSC curves were obtained on a Netzsch DSC 204 F1 apparatus. The measuring system was calibrated according to ISO 11357-1 standard by the temperatures and enthalpies of phase transitions of standard substances (listed in Table 1). Samples were put in aluminum crucibles with pierced lid (V=40 mm^3, d=6 mm) in the flow (40 ml/min) of dried nitrogen (99.998 vol%). The measurements were held in the 188.15-298.15 K temperature range at heating rate 2 K/min. Cooling experiments were not held due to formation of supercooled liquid. The masses of the samples were within the 2-8 mg range. Standard uncertainty of melting point temperatures and heats of fusion in DSC curves was ±1 K and ±5.0%, respectively. A solidus temperature for a sample was assessed as an extrapolated onset temperature of the first DSC peak, a liquidus temperature - as the last peak temperature corrected on a thermal resistance

[9,10]. The enthalpy of fusion of pure substances was defined as an area between peak and interpolated baseline. Software package NETZSCH Proteus Thermal Analysis was employed for experimental data processing. Some of DSC curves are presented in Fig. 1.

THERMODYNAMIC MODELING

1. Literature Data

One of the most popular EoS used to describe the properties of substances and their mixtures (liquid and vapor) is the cubic equation of state. Advantages of this type of EoS are relative simplicity, high speed of calculation and applicability to describe properties in a wide range of temperature and pressure. Parameters of cubic EoS can be calculated from the condition for a critical point. Unfortunately, this way of calculation does not lead to correct description of the *P-v-T* properties of individual substances away from the critical point; therefore, parameters were fitted to experimental *P-v-T* data. Initial approximation for critical temperatures was found in the literature [11,12], critical pressures were calculated according Joback's group contribution method [13], acentric factors were estimated by Edmister formula [14]. These data are shown in Table 2.

Literature data on *P-v-T* properties of *o*-DCB - *m*-DCB system were gathered and analyzed. Whereas data on pure substances are sufficient for calculations (see Table 3), data on mixtures contain only excess volumes (v^E) measured at one temperature (298 K). Note that the values of excess volumes are small; thus, behavior of the investigated system is close to the ideal.

Data on isobaric liquid heat capacity and isobaric ideal gas heat capacity are also necessary for *h-P* diagram calculations (see Supplementary material). Liquid heat capacities of *o*-DCB and *m*-DCB were found in the literature, gas heat capacity was estimated by Joback's group contribution method [13]. Expression for gas heat capacity of *o*-DCB and *m*-DCB was found to be

$$C_p^{gas}=3.61+0.449T-3.0756\cdot10^{-4}T^2+7.88\cdot10^{-8}T^3\ [J/(mol\cdot K)]. \quad (2)$$

Solid-liquid equilibria in this system were not investigated before. Data on points and heats of fusion of pure *o*-DCB and *m*-DCB are presented in [43,48,56-62] (Table 4). Experimental values were received by DSC method. Results of different authors coincide well with each other except [61] that can be explained by existence of impurities in used reagents.

Vapor-liquid equilibria in this system also were not investigated before. Data on normal boiling point of pure *o*-DCB and *m*-DCB were found in [20,24,63-66] (Table 5). Most of the sources are handbooks, where experimental methods and purity of used reagents are not mentioned. However, all data coincide with each other well. Detailed description of method and information about reagents is presented only for *o*-DCB in [66], also including data on boiling points at 300, 500 and 700 mmHg.

Table 2. Literature data on critical parameters and acentric factors of *o*- and *m*-DCB

Substance	T_c, K	P_c, bar	ω
o-DCB	698.8 [11]	41.52 [13]	0.273 [14]
m-DCB	685.7 [12]	41.52 [13]	0.219 [14]

Table 3. Experimental data on the properties of the *o*-DCB - *m*-DCB system

Data type	Chemical	T, K	N[a]	Ref.
ρ^L	*o*-DCB	298-338	53	[15-37]
	m-DCB	251-409	52	[26-42]
	o-DCB - *m*-DCB	288-318	36	This work
P^{sat}	*o*-DCB	256-455	89	[26,43-51]
	m-DCB	249-448	79	[26,46-52]
v^E	*o*-DCB - *m*-DCB	298	21	[53]
C_p^L	*o*-DCB	263-377	56	[28,54,55]
	m-DCB	263-378	64	[28,54,55]

[a]N - number of experimental points.

2. Equation of State

The most famous and successful cubic equations of state used in thermodynamic calculations are the Soave-Redlich-Kwong [67] and Peng-Robinson EoS [68]. These equations show good results even for mixtures of polar substances when they are used to describe vapor pressure. However, they predict unsatisfactory volumetric properties (density of liquids) [69]. This behavior was also observed in calculations for the investigated system. One of the approaches to improve description of liquid densities is to introduce correction to the molar volume: molar volume calculated from the Soave or Peng-Robinson EoS v_{EoS} is corrected by subtracting a parameter c; this idea was proposed by Péneloux in 1982 [70]. Equations of state

Table 4. Literature data on temperatures and heats of fusion of *o*-DCB and *m*-DCB

Substance	T_m, K	ΔH_m, kJ/mol
o-DCB	256,15 [43], 256,12 [48], 256,45 [56], 255,85±0,2 [57], 256,0 [58], 255,65 [59], 256,15±0,1 [60], 253,91 [61], 256,14±0,1 [62]	12,93 [56], 13,09±0,4 [57], 12,92 [58]
m-DCB	248,39 [48], 248,35 [56], 248,25±0,2 [57], 249,0 [58], 248,75 [59]	12,64 [56], 12,51±0,4 [57], 12,59 [59]

Table 5. Literature data on normal boiling points of *o*-DCB and *m*-DCB

Substance	T_b, K
o-DCB	453,65 [20], 453,35 [24], 453,6 [63], 453,55 [64], 453,55 [65], 453,4 [66]
m-DCB	446,25 [20], 445,55 [24], 446,1 [63], 446,15 [64], 445,95 [65]

including such correction are called volume-translated equations of state, VT-EoS.

$$v_{VT-EoS}=v_{EoS}-c \tag{3}$$

Review [71] contains various expressions for the correction c to the Peng-Robinson equation of state, generally having advantages over the Soave EoS. For example, the equation of state proposed by Tsai and Chen [72] showed excellent results for more than 100 polar and non-polar compounds. Authors offer to use temperature-dependent α-function:

$$\alpha(T)=[1+M^*(1-T_r)+N^*(1-T_r)(0.7-T_r)]^2, \tag{4}$$

where M^* and N^* - individual parameters of pure fluid. Parameter M is correlated as a function of acentric factor:

$$M^*=0.20473+0.83548\omega-0.18470\omega^2+0.16675\omega^3-0.09881\omega^4 \tag{5}$$

Volume correction c is evaluated by the following formula:

$$c=\frac{RT_c}{P_c}[k_1+k_2(1-T_r^{2/3})+k_3(1-T_r^{2/3})^2]^2, \tag{6}$$

It was found that k_1 can be expressed as a function of acentric factor, k_2 can be regressed as a function of k_3:

$$k_1=0.00185+0.00438\omega+0.36322\omega^2-0.90831\omega^3+0.55885\omega^4 \tag{7}$$

$$k_2=-0.00542-0.51112k_3+0.04533k_3^2+0.07447k_3^3-0.03831k_3^4 \tag{8}$$

Thus, Tsai-Chen EoS contains two pure fluid parameters N^* and k_3, in addition to the critical properties and acentric factor. This equation of state was implemented for calculations in this work.

3. Calculation Procedure

The critical parameters, acentric factors and additional parameters N and k_3 allowed us to evaluate the values of parameters a, b and c for experimental temperatures. Then, Tsai-Chen EoS was considered as a cubic equation of the compressibility factor:

$$Z^3-(1-BC)Z^2+(A-3B^2-2B+3C^2+2BC-2C)Z - (AB-B^2-B^3-C^3-BC^2+3B^2C+C^2+2BC-AC)=0, \tag{9}$$

where $A=aP/(RT)^2$, $B=bP/(RT)$, $C=cP/(RT)$.

A cubic equation has one or three real solutions. One real root means that system is a single-phase, and the root corresponds to the compressibility factor of this phase. If the equation has three real roots, solutions should be checked. It is necessary to calculate Gibbs energies of phases relative to a reference state - ideal gas at 1 bar:

$$g(T, P)-g(T, P^0)=RT\ln\frac{f}{f^0}, \tag{10}$$

where f - fugacity, $P^0=f^0=1$ bar. If Gibbs energies of phases are equal, the system is two-phase at this temperature and pressure, the smallest value of compressibility factor corresponds to liquid, the largest - to vapor, the middle one does not have a physical meaning. If Gibbs energy of one phase is larger than of another, system is one-phase, Z-factor of phase is equal to Z-factor of phase with the least value of Gibbs energy.

It is possible to calculate liquid density and fugacity coefficients from the compressibility factor values:

$$v^L=\frac{Z^LRT}{P};\ \rho^L=\frac{M}{v^L} \tag{11}$$

$$\ln\varphi=Z+C-1-\ln(Z+C-B)-\frac{A}{2\sqrt{2}B}\ln\left(\frac{Z+C+(1+\sqrt{2})B}{Z+C+(1-\sqrt{2})B}\right) \tag{12}$$

The fugacity coefficients were used to calculate the saturated vapor pressure from the equilibrium condition between liquid and vapor phases:

$$f^V(T_{exp}, P^{sat})=f^L(T_{exp}, P^{sat}) \tag{13}$$

The parameters was calculated by minimizing the objective function using the trust-region-reflective algorithm. The objective function was the sum of squared relative deviations of calculated liquid densities and saturated vapor pressures from experimental ones:

$$F=\sum_{i=1}^{n}e_i^2=\sum\left(\frac{\rho^L_{calc}-\rho^L_{exp}}{\rho^L_{exp}}\right)^2+\sum\left(\frac{P^{sat}_{calc}-P^{sat}_{exp}}{P^{sat}_{exp}}\right)^2, \tag{14}$$

where $e_i=\frac{X_{i,\,calc}-X_{i,\,exp}}{X_{i,\,exp}}$ is relative deviation of *i*-th experimental point of property X; summation was held for all experimental values of density of liquid and saturated vapor pressure of pure substances (see Table 3); subscripts «calc» and «exp» refer to calculated and experimental values respectively.

Determination of EoS parameters of pure substances (T_c, P_c, ω, N^*, k_3) allowed calculating EoS parameters of mixtures. Excess volumes [53] and liquid densities measured in this work (volumetric properties) were used as input data to calculate of EoS parameters for mixtures. Densities of liquid were calculated from literature data on excess volumes by following formula:

$$\rho^L=\frac{M}{M\cdot\left(\frac{z_1}{\rho_1}+\frac{z_2}{\rho_2}\right)+v^E}, \tag{15}$$

where z_1 and z_2 - molar fractions of *o*-DCB and *m*-DCB in mixtures, ρ_1 and ρ_2 - densities of pure liquid *o*-DCB and *m*-DCB, M - molar mass of dichlorobenzenes.

The procedure of EoS parameters evaluation for mixtures was almost the same as for pure substances. The only difference was a mixing rule needed to calculate the EoS parameters of mixtures. In this work, the van der Waals mixing rule was used: quadratic rule for parameter a, linear rule for parameter b:

$$a=\sum_i\sum_j z_iz_ja_{ij},\ a_{ij}=\sqrt{a_ia_j}(1-k_{ij}) \tag{16}$$

$$b=\sum_i z_ib_i \tag{17}$$

For volume correction c it is recommended to use linear mixing rule [72]:

$$c=\sum_i z_ic_i \tag{18}$$

After the EoS parameters evaluation, it became possible to calculate properties of the considered system: enthalpy, entropy and density. These properties are conveniently represented as a diagram in the enthalpy–pressure coordinates.

Initially, the vapor-liquid equilibria (VLE) problem was solved by

a two-phase flash calculation. Calculation procedure used in the work was the same as reported in [73,74]. Input data were temperatures, pressures and overall compositions of the system. Calculation procedure included Michelsen stability test for liquid and vapor phases and solving of Rachford-Rice equation by substitution-type method. Result of the calculation is compositions of equilibrium phases.

Enthalpy, entropy and density of the system were calculated to construct an *h-P* diagram. Possible routes for enthalpy calculations are presented in [69]. In this work, the route with liquid as an initial phase was chosen. The calculations were held for the T=280÷680 K with step 40 K and for the P=e^7÷e^{16} Pa with step (e^{16}−e^7)/1,000 Pa. This range of temperatures and pressures includes the conditions most commonly used in power plants working on Rankine cycle. The enthalpy calculation was carried out using standard enthalpies of the formation of liquid *o*-DCB and *m*-DCB at T^0=298.15 K and P^0=1 bar as the reference level taken equal to zero. Detailed route of calculations is presented in Appendix A.

RESULTS AND DISCUSSION

1. Pure Substances

All the data on properties of pure *o*-DCB and *m*-DCB that were used for modeling are summarized in Table 6.

Data on saturated vapor pressure of *o*-DCB and *m*-DCB are presented in [26,43-52]. In article [51], the authors collected all the available data on saturated vapor pressure of *o*-DCB and *m*-DCB and analyzed them. The data [44,45] obtained by the gas saturation-GC method, data [46] obtained by pressure gauge method and the data presented in the review [47] diverge greatly from the experimental values recommended by the authors from articles [49,50]. This fact was explained by the inconsistency of the data [44-47] with the available thermochemical data. Therefore, in this work, only data from sources [26,43,48-52] were used for calculations.

Experimental data on saturated vapor pressure and results of their estimation by Tsai-Chen EoS are presented in Fig. 2 and Table 4. Due to α-function, Tsai-Chen EoS is able to describe saturated vapor pressure of pure substances within experimental uncertainty.

Results of the density description by the model are shown in Fig. 3 and Table 6. It can be seen that existing experimental data are consistent, obtained model parameters describe well all of the data on the density of pure substances. Tsai-Chen EoS contains five parameters, which are enough to describe liquid density with high accuracy. Deviations of calculated liquid densities from the experiment values do not exceed 0.5%.

Obtained parameters of Tsai-Chen EoS with their confidence intervals are listed in Table 7. All parameters are statistically significant. Moreover, the equation of state has physically correct behavior. It evaluates correctly thermodynamic properties of pure *o*-DCB and *m*-DCB from melting point to boiling point.

2. Mixtures

Results of the density measurements of *o*-DCB - *m*-DCB solutions at 288.15, 298.15, 308.15 and 318.15 K are listed in Table 8.

Table 6. Experimental data used for modeling the pure substances in the *o*-DCB - *m*-DCB system and results of their description

Substance	Data type	Ref.	N	T, K	MRD[a], %
o-DCB	ρ^L	[15-37]	53	298-338	0.36
	P^{sat}	[26,43,48-51]	63	256-455	3.0
m-DCB	ρ^L	[26-42]	52	251-409	0.32
	P^{sat}	[26,48-52]	65	249-448	2.8

[a]Maximum relative deviation MRD (X), %= $\max\left(\left|\frac{X_{calc}-X_{exp}}{X_{exp}}\right|\right)\times 100$, where X_{calc} and X_{exp} are the calculated and experimental values.

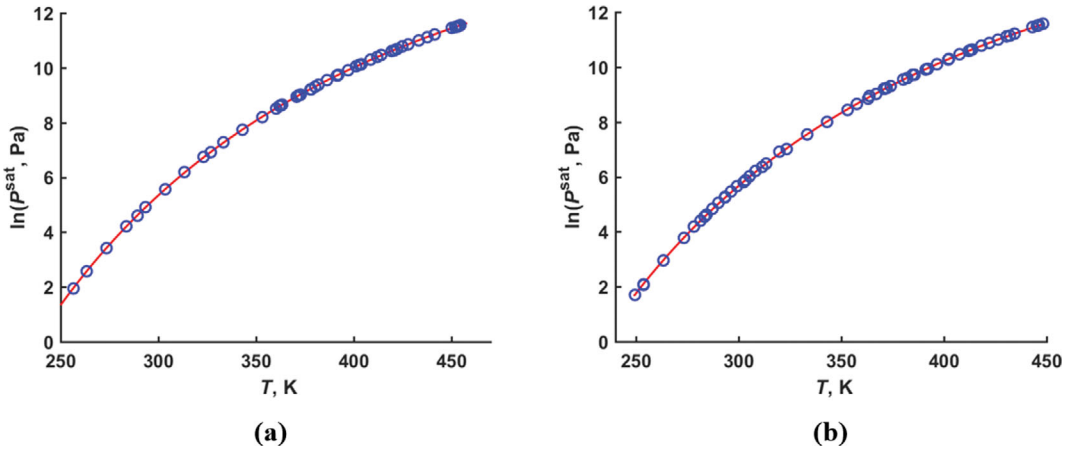

Fig. 2. Saturated vapor pressure of the (a) pure *o*-DCB, (b) pure *m*-DCB. Red line - calculations by the obtained model; blue circles - literature data [26,43,48-52].

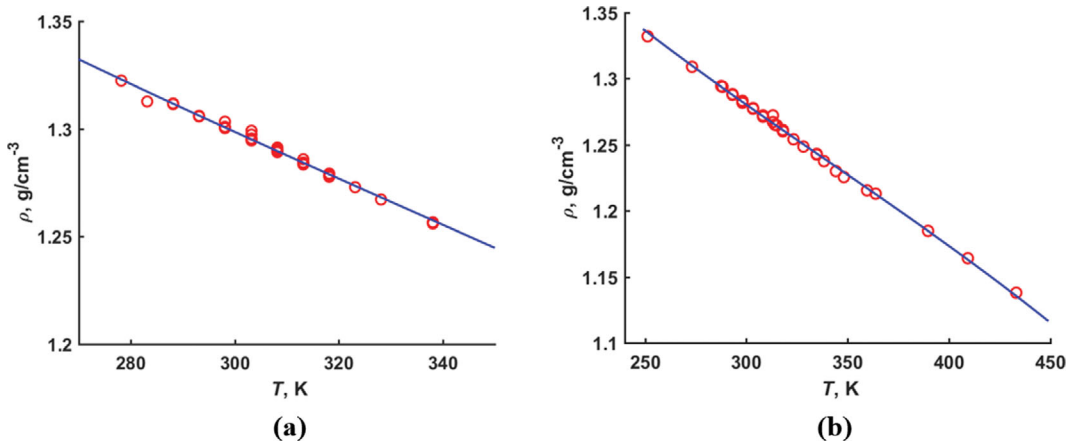

Fig. 3. Liquid density of the (a) pure *o*-DCB, (b) pure *m*-DCB. Blue line - calculations by the obtained model; red circles - literature data [15-42].

Table 7. Tsai-Chen EoS parameters with 95% confidence intervals for the *o*-DCB - *m*-DCB system

	T_c, K	P_c, bar	ω	N	k_3
o-DCB	726.2±8.1	44.33±1.55	0.138±0.028	0.407±0.023	0.056±0.030
m-DCB	724.9±16.9	45.01±2.74	0.096±0.058	0.441±0.050	0.056±0.031

Table 8. Densities of the binary solutions in the *o*-dichlorobenzene - *m*-dichlorobenzene system at various temperatures and pressure 100 kPa

w(*m*-DCB)	$\rho_{288.15\,K}$, g/cm^{-3}	$\rho_{298.15\,K}$, g/cm^{-3}	*w*(*m*-DCB)	$\rho_{308.15\,K}$, g/cm^{-3}	$\rho_{318.15\,K}$, g/cm^{-3}
9.97	1.3096	1.2985	10.01	1.2878	1.2764
20.11	1.3086	1.2974	20.02	1.2861	1.2748
30.74	1.3068	1.2955	30.04	1.2843	1.2729
39.88	1.3050	1.2936	40.00	1.2826	1.2713
50.27	1.3033	1.2919	50.07	1.2808	1.2694
60.00	1.3015	1.2899	60.04	1.2790	1.2676
70.26	1.2999	1.2882	69.97	1.2772	1.2658
80.66	1.2980	1.2863	80.03	1.2754	1.2640
86.81	1.2961	1.2845	89.79	1.2734	1.2621

Standard uncertainties: u(P)=1 kPa, u(T)=0.02 K, $u_r(w)$=0.002, $u_r(\rho)$=0.002; u_r - relative standard uncertainty, w - mass fraction in %.

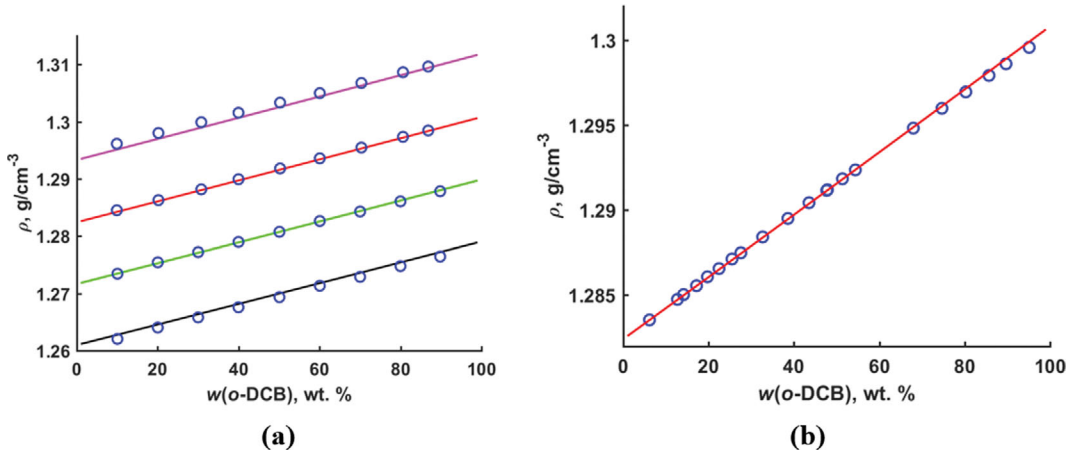

Fig. 4. Liquid density of *o*-DCB - *m*-DCB mixtures: (a) measured in this work at 288.15, 298.15, 308.15 and 318.15 K; (b) calculated from excess volumes measured at 298.15 K in [53]. Purple, red, green and black lines - calculations by the obtained model at 288.15, 298.15, 308.15 and 318.15 K, respectively; blue circles - experimental data [this work, 53].

Table 9. Experimental data used for modeling the mixtures in the *o*-DCB - *m*-DCB system and results of their description

Data type	Ref.	N	T, K	MRD, %
v^E	[53]	21	298	0.026
ρ^L	[This work]	36	288-318	0.063

Table 10. Coordinates of solidus (T_s) and liquidus (T_l) of the *o*-DCB - *m*-DCB system at the pressure P=100 kPa and areas ($S_{1/2}$) for the determination of eutectic composition in *o*-DCB - *m*-DCB system by «enthalpic» method [75]

w^a(*m*-DCB), wt%	T_s^b, K	T_l^c, K	$S_{1/2}{}^d$, J/g
0	-	256.1	0
10.14	225.1	251.7	8.96
19.73	225.3	245.3	18.13
20.25	225.5	245.8	18.06
30.02	225.5	240.9	22.95
40.02	225.5	233.0	40.15
50.02	224.4	-	51.28
59.04	224.5	-	49.05
69.92	225.5	233.8	28.79
79.56	225.6	239.4	22.14
90.03	225.4	244.7	10.2
100	-	248.4	0

Standard uncertainties: u(P)=1 kPa, ^{a}u$_r$(w)=0.01, ^{b}u(T_s)=0.2 K, ^{c}u(T_l)=1 K, ^{d}u($S_{1/2}$)=0.005.

Based on experimental data on volumetric properties of mixtures, the parameters of the EoS for mixtures were determined under the assumption of equality to zero of the binary interaction coefficient k_{ij} (16). Results of the density description of *o*-DCB - *m*-DCB solutions by the model are shown in Fig. 4, maximum relative deviations of calculated liquid densities from experimental values are shown in Table 9. Relative deviations do not exceed 0.1%. Therefore, the simplest mixing rule allowed predicting densities of the mixtures precisely.

However, to check if it is possible to improve accuracy of the model, the binary interaction coefficient was set as variable in minimization. Its value was very close to zero, but more than that, the parameter was statistically insignificant. Therefore, the assumption was correct and in the next calculations the parameter k_{ij} was taken equal to zero.

Data on solid-liquid phase equilibria (SLE) make possible to determine the lower bound of the temperature range in which the liquid can be stored and used. If the assumption of ideal mixing is correct, predicted solid-liquid equilibria will be in a good agreement with an experiment. SLE was studied by differential scanning calorimetry (DSC). Results of DSC measurements are presented in Table 10.

The melting parameters obtained in this work are well consistent with the data presented in the literature (Table 11).

DSC peaks for compositions next to the eutectic point are overlapped so their separation and quantitative estimation of transition temperatures are difficult. Therefore, the eutectic composition was

Table 11. Melting parameters of *o*-DCB and *m*-DCB

Substance	T_m, K	Δh_m, kJ/mol
o-DCB	256.45 [56]	12.93 [56]
	255.85±0.2 [57]	13.09±0.4 [57]
	256.1±0.1 [this work]	13.2±0.5 [this work]
m-DCB	248.35 [56]	12.64 [56]
	248.25±0.2 [57]	12.51±0.4 [57]
	248.4±0.1 [this work]	13.3±0.5 [this work]

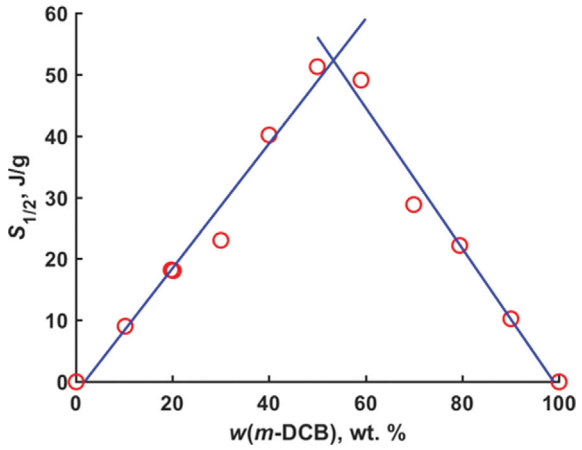

Fig. 5. An illustration of «enthalpic method» to determine an eutectic point for the *o*-DCB - *m*-DCB system.

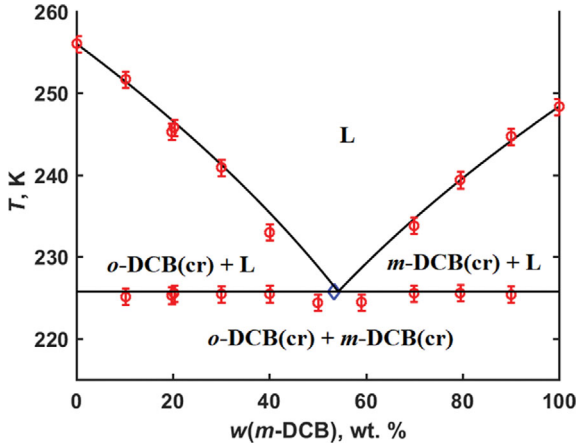

Fig. 6. Isobaric phase diagram (P=100 kPa) of the *o*-DCB - *m*-DCB system at 215-260 K: red circles - experimental values, blue diamond - estimation of eutectic composition by «enthalpic» method, lines - calculation under the assumption of an ideal solution, L - liquid phase.

evaluated by so-called «enthalpic» method [75]. This composition was found as the coordinate of the intersection of two lines, describing the dependence of the enthalpic fraction of solidus melting from the mixture composition (Fig. 5).

The resulting equations for lines are:

$$S_{1/2}=1.02w-1.9 \quad (19)$$

$$S_{1/2}=-1.15w+113.4 \quad (20)$$

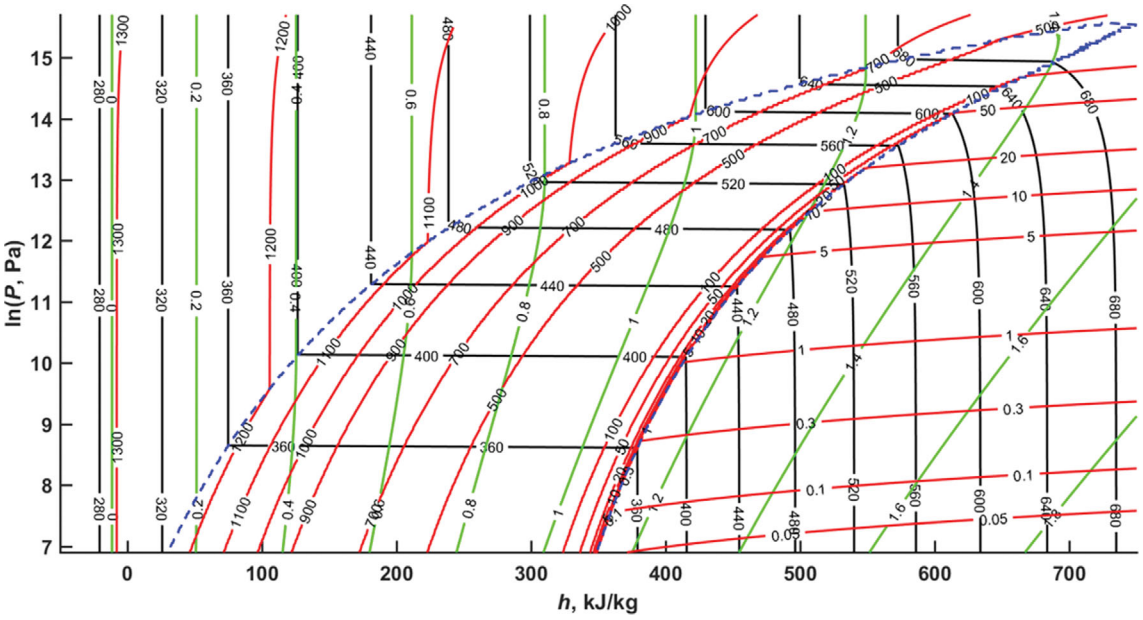

Fig. 7. *h-P* diagram calculated for the mixture of *o*-dichlorobenzene - *m*-dichlorobenzene: *w*(*o*-DCB)=55 wt%, *w*(*m*-DCB)=45 wt%. Black lines - isotherms (values on lines in K), green lines - isentropic (values on lines in kJ/kg/K), red lines - lines of equal density (values on lines in kg/m^3), dashed blue line restricts vapor-liquid region.

where w is *m*-DCB mass fraction percent (wt%) and $S_{1/2}$ is the resulting partial area of the solidus peak (from onset to maximum temperature) divided by sample mass (J/g). The predicted eutectic composition is (53.3±1.5) wt% *m*-DCB.

Melting points and heats of fusion of individual substances were used as stability parameters to calculate the phase diagram (Fig. 6). The liquid phase was supposed to be an ideal solution. The resulting diagram relates to a simple eutectic type. Results of DSC measurements for mixtures were compared with the calculated phase diagram. On average, the calculated liquidus and solidus deviate from experimental ones less than for 1 K. Maximum deviations do not exceed 1.5 K for solidus, 2.5 K for liquidus. The eutectic composition found by the «enthalpic» method is also in a good agreement with the results of calculations (difference is less than 1 wt%).

Finally, the *h-P* diagram was calculated (Fig. 7). As an example, overall composition of the system is the following: *w*(*o*-DCB)=55 wt%, *w*(*m*-DCB)=45 wt%. The diagram can be used to estimate energy efficiency of plants operating on the Rankine cycle with an *o*-dichlorobenzene - *m*-dichlorobenzene working body of given composition.

CONCLUSIONS

Literature data on thermodynamic properties and phase equilibria in the *o*-dichlorobenzene - *m*-dichlorobenzene system were gathered and analyzed. Based on critical properties and thermodynamic properties of pure substances, a cubic equation of state of was proposed. As was revealed, Soave-Redlich-Kwong and Peng-Robinson EoS could not describe correctly volumetric properties of the pure substances. The best results were achieved with Tsai-Chen EoS.

Experimental measurements of volumetric properties of solutions at 288.15, 298.15, 308.15 and 318.15 K by vibrating-tube densimeter were performed to obtain EoS parameters of mixtures. Liquid densities of mixtures were correctly predicted within the ideal assumption. Solid-liquid equilibria of *o*-dichlorobenzene - *m*-dichlorobenzene at P=1 bar (100 kPa) were studied by DSC, composition of eutectic point was evaluated by «enthalpic» method. Phase diagram of the system in SLE range was calculated assuming liquid as ideal solution. The resulting diagram is in a good agreement with experimental data on SLE.

A *h-P* diagram for an *o*-dichlorobenzene - *m*-dichlorobenzene mixture with composition *w*(*o*-DCB)=55 wt%, *w*(*m*-DCB)=45 wt% was calculated using the resulting EoS. The diagram can be used to estimate energy efficiency of plants operating on the Rankine cycle with an *o*-dichlorobenzene - *m*-dichlorobenzene working body.

ACKNOWLEDGEMENTS

This study was performed in the frame of theme «Chemical Thermodynamics and Theoretical Material Science».

NOMENCLATURE

a : parameter of equation of state [Pa·m^6/mol^2]
a_i : parameter of equation of state for pure component [Pa·m^6/mol^2]
a_{ij} : interaction parameters for mixture [Pa·m^6/mol^2]
A : dimensionless parameter [-]
A* : calibration coefficient
b : parameter of equation of state [m^3/mol]
b_i : parameter of equation of state for pure component [m^3/mol]
B : dimensionless parameter [-]
B* : calibration coefficient
c : parameter of equation of state [m^3/mol]

c_i : parameter of equation of state for pure component [m^3/mol]
cr : crystal
C : dimensionless parameter [-]
C_p : isobaric heat capacity [J/(mol·K)]
DSC : signal in differential scanning calorimetry [mW/mg]
f : fugacity [Pa]
g : Gibbs energy of phase [J/mol]
h : enthalpy [kJ/kg]
k_1 : parameter in Eq. (15)
k_2 : parameter in Eq. (15)
k_3 : parameter in Eq. (15)
k_{ij} : binary interaction parameter [-]
m : multiplier in expression for alpha-function [-]
M : molecular weight [g/mol]
M^* : individual parameter of fluid [-]
MRD : maximum relative deviation [%]
N : number of data points [-]
N^* : individual parameter of fluid [-]
P : pressure [Pa]
P^{sat} : pressure of saturated vapor [Pa]
R : gas constant [J/(K*mol)]
$S_{1/2}$: half-area of solidus peak [J/g]
T : absolute temperature [K]
T_l : liquidus temperature [K]
T_m : melting point [K]
T_r : reduced temperature [-]
T_s : solidus temperature [K]
u : standard uncertainty
v : molar volume [m^3/mol]
v^E : excess volume of a mixture [m^3/mol]
w : mass fraction [%]
z : mole fraction [%]
Z : compressibility factor [-]
α : alpha-function [-]
ρ : density of liquid [g/ml]
τ : oscillation period [ms]
φ : fugacity coefficient [-]
ω : acentric factor [-]
Δh_m : enthalpy of fusion [kJ/mol]

Subscripts

1 : component 1
2 : component 2
c : critical property
calc : calculated
exp : experimental
i : component i
j : component j
r : relative
EoS : equation of state
VT−EoS : volume-translated equation of state

Superscripts

L : liquid
V : vapor
0 : reference state

SUPPORTING INFORMATION

Additional information as noted in the text. This information is available via the Internet at http://www.springer.com/chemistry/journal/11814.

REFERENCES

1. M. Moran, H. Shapiro, D. Boettner and M. Bailey, *Fundamentals of engineering thermodynamics*, 8th ed., Wiley, Hoboken (2014).
2. K. Sipilä, *Advanced District Heating and Cooling (DHC) Systems. Chapter 3 - Cogeneration, biomass, waste to energy and industrial waste heat for district heating*, 1st ed., Woodhead Publishing, Cambridge (2016).
3. G. Belov and M. Dorokhova, *Sci. Educ. Bauman MSTU.*, **14**, 99 (2014).
4. V. Pethurajan, S. Sivan and G. C. Joy, *Energy Convers. Manag.*, **166**, 474 (2018).
5. N. A. Lai, M. Wendland and J. Fischer, *Energy*, **36**, 199 (2011).
6. U. Drescher and D. Bru, *Appl. Therm. Eng.*, **27**, 223 (2007).
7. C. Sprouse and C. Depcik, *Appl. Therm. Eng.*, **51**, 711 (2013).
8. M. Holik, M. Živić, Z. Virag, A. Barac, M. Vujanović and J. Avsec, *Energy Convers. Manag.*, **232**, 113897 (2021).
9. D. A. Kosova, A. L. Voskov, N. A. Kovalenko and I. A. Uspenskaya, *Fluid Phase Equilib.*, **425**, 312 (2016).
10. E. V. Belova, V. S. Krasnov, A. B. Ilyukhin and I. A. Uspenskaya, *Thermochim. Acta*, **668**, 46 (2018).
11. C. L. Young, C. A. Tran and D. W. Morton, *J. Chem. Eng. Data*, **62**, 2953 (2017).
12. D. W. Morton, M. P. W. Lui, C. A. Tran and C. L. Young, *J. Chem. Eng. Data*, **45**, 437 (2000).
13. B. E. Poling and J. M. Prausnitz, *The properties of gases and liquids*, 5th ed., McGraw-Hill, New York (2001).
14. R. Reid, J. Prausnitz and T. Sherwood, *The properties of gases and liquids*, 4th ed., McGraw-Hill, New York (1977).
15. K. Dayananda Reddy, M. Prabhakara Rao and M. Ramakrishna, *Phys. Chem. Liq. An Int. J.*, **15**, 59 (1985).
16. A. J. Easteal, P. J. Back and L. A. Woolf, *J. Chem. Eng. Data*, **42**, 1261 (1997).
17. J. Sekar, P. Naidu and J. W. Acree, *J. Chem. Eng. Data*, **38**, 167 (1993).
18. S. S. Yadava, S. Singh, R. Bhan and N. Yadav, *Korean J. Chem. Eng.*, **28**, 256 (2011).
19. S. S. Yadava, R. Bhan and N. Yadav, *J. Solution Chem.*, **41**, 926 (2012).
20. R. R. Dreisbach, *Physical properties of chemical compounds. advances in chemistry*, Vol. 15, American Chemical Society, Washington (1961).
21. J. G. Baragi, M. I. Aralaguppi, T. M. Aminabhavi, M. Y. Kariduraganavar and S. S. Kulkarni, *J. Chem. Eng. Data*, **50**, 917 (2005).
22. W.-M. Melzer, W. Baldauf and H. Knapp, *Chem. Eng. Process. Process Intensif.*, **26**, 71 (1989).
23. R. Raju, S. Ravikumar, K. Sivakumar, M. Raveendra and V. Pandiyan, *Chem. Data Collect.*, **17-18**, 41 (2018).
24. W. Haynes, D. Lide and T. Bruno, *CRC handbook of chemistry and physics*, 95th ed., CRC PRESS, Boca Raton (2014).
25. V. Syamala, D. Sekhar, K. Sivakumar and P. Venkateswarlu, *Phys. Chem. Liq. An Int. J.*, **48**, 171 (2010).

26. K. Ramanjaneyulu, A. Krishnaiah and M. Ramakrishna, *Fluid Phase Equilib.*, **40**, 311 (1988).
27. S. C. Bhatia, J. Sangwan, R. Rani and R. Bhatia, *Int. J. Thermophys.*, **32**, 2027 (2011).
28. P. Góralski and H. Piekarski, *J. Chem. Eng. Data*, **52**, 655 (2007).
29. P. M. Reddy, K. Siva and P. Venkatesu, *Fluid Phase Equilib.*, **310**, 74 (2011).
30. M. M. Mato, J. Balseiro, J. Salgado, E. Jime, L. Legido, M. M. Pin, F. De Ciencias and E.-A. Corun, *J. Chem. Eng. Data*, **47**, 4 (2002).
31. G. P. Chand, M. G. Sankar, P. N. V. V. L. P. Rani and C. Rambabu, *J. Mol. Liq.*, **201**, 1 (2015).
32. P. V. Rao, T. S. Krishna, M. Gowri and K. Ravindhranath, *J. Mol. Liq.*, **222**, 873 (2016).
33. V. Syamala, K. S. Kumar and P. Venkateswarlu, *J. Chem. Thermodyn.*, **38**, 1553 (2006).
34. V. Syamala, L. Venkatramana, C. N. Rao, K. Sivakumar, P. Venkateswarlu and R. L. Gardas, *Fluid Phase Equilib.*, **397**, 68 (2015).
35. P. Vasundhara, C. N. Rao, L. Venkatramana, K. Sivakumar, P. Venkateswarlu and R. L. Gardas, *J. Mol. Liq.*, **202**, 158 (2015).
36. L. Venkatramana, K. Sivakumar, V. Govinda and K. D. Reddy, *J. Mol. Liq.*, **186**, 163 (2013).
37. G. Towler and R. Sinnott, *Chemical engineering design principles, practice and economics of plant and process design*, Butterworth-Heinemann, Oxford (2012).
38. F. M. Jaeger, *Zeitschrift Für Anorg. Und Allg. Chemie.*, **101**, 1 (1916).
39. V. C. Kumar, B. Sreenivasulu and P. R. Naidu, *J. Chem. Eng. Data*, **38**, 414 (1993).
40. J. Rajasekar and P. R. Naidu, *J. Chem. Eng. Data*, **41**, 373 (1996).
41. J. Rajasekhar and K. Sivakumar, *Fluid Phase Equilib.*, **245**, 149 (2006).
42. A. Vogel, *J. Chem. Soc.*, 644 (1948).
43. R. McDonald, S. Shrader and D. Stull, *J. Chem. Eng. Data*, **4**, 311 (1959).
44. B. T. Grayson and L. A. Fosbraey, *Pestic. Sci.*, **13**, 269 (1982).
45. K. Liu and R. M. Dickhut, *Chemosphere*, **29**, 581 (1994).
46. C. F. Fisk and W. A. Noyes, *J. Am. Chem. Soc.*, **58**, 1707 (1936).
47. D. R. Stull, *Ind. Eng. Chem.*, **39**, 517 (1947).
48. R. R. Dreisbach and S. A. Shrader, *Ind. Eng. Chem.*, **41**, 2879 (1949).
49. M. Poledníček, T. Guetachew, J. Jose, V. Růžička, V. Roháč and M. Zábranský, *ELDATA: The Int. Electron. J. Physico-Chemical Data*, **2**, 41 (1996).
50. V. Roháč, V. Růžička, K. Růžička and K. Aim, *J. Chem. Eng. Data*, **43**, 770 (1998).
51. D. Mackay, W. Y. Shiu, K. C. Ma and S. C. Lee, *Handbook of physical-chemical properties and environmental fate for organic chemicals: Volume I: Introduction and hydrocarbons*, CRC Press, Boca Raton (2006).
52. S. P. Verevkin, V. N. Emel'yanenko, M. A. Varfolomeev, B. N. Solomonov, K. V. Zherikova and S. V. Melkhanova, *J. Phys. Chem. B*, **118**, 14479 (2014).
53. R. Tanaka and G. C. Benson, *J. Chem. Eng. Data*, **24**, 37 (1979).
54. M. Lipovská, H. G. Schmidt, V. Roháč, V. Růžička, G. Wolf and M. Zábranský, *J. Therm. Anal. Calorim.*, **68**, 753 (2002).
55. V. Roháč, V. Růžička, K. Růžička, M. Poledníček, K. Aim, J. Jose and M. Zábranský, *Fluid Phase Equilib.*, **157**, 121 (1999).
56. W. E. Acree, *Thermochim. Acta*, **189**, 37 (1991).
57. D. Wei, *Thermochim. Acta*, **479**, 32 (2008).
58. J. Timmermans, *Bull. Soc. Chim. Belg.*, **44**, 17 (1935).
59. J. Narbutt, *Z. Elektrochem.*, **24**, 339 (1918).
60. U. Domańska and T. M. Letcher, *J. Chem. Thermodyn.*, **32**, 1635 (2000).
61. J. R. Donnelly, L. A. Drewes, R. L. Johnson, W. D. Munslow, K. K. Knapp and G. W. Sovocool, *Thermochim. Acta*, **167**, 155 (1990).
62. C. R. Witschonke, *Anal. Chem.*, **26**, 562 (1954).
63. P. Basařová and V. Svoboda, *Fluid Phase Equilib.*, **68**, 13 (1991).
64. R. M. Stephenson and S. Malanowski, *Handbook of the thermodynamics of organic compounds*, Elsevier, New York (1987).
65. Physical Property Data Bank. Appendix C.
66. R. Kalluru and K. Abburi, *Fluid Phase Equilib.*, **40**, 311 (1988).
67. G. Soave, *Chem. Eng. Sci.*, **27**, 1197 (1972).
68. D.-Y. Peng and D. B. Robinson, *Ind. Eng. Chem., Fundam.*, **15**, 59 (1976).
69. J. Gmehling, M. Kleiber, B. Kolbe and J. Rarey, *Chemical thermodynamics for process simulation*, 2nd ed., Wiley, New Jersey (2019).
70. A. Péneloux, E. Rauzy and R. Fréze, *Fluid Phase Equilib.*, **8**, 7 (1982).
71. F. Young, F. L. P. Pessoa and V. R. R. Ahón, *Fluid Phase Equilib.*, **435**, 73 (2017).
72. J.-C. Tsai and Y.-P. Chen, *Fluid Phase Equilib.*, **145**, 193 (1998).
73. C. H. Whitson and M. Brulé, *Phase behavior*, Henry L. Doherty Memorial Fund of AIME, Society of Petroleum Engineers, Richardson (2000).
74. https://www.e-education.psu.edu/png520/.
75. M. S. Ding, K. Xu and T. R. Jow, *J. Therm. Anal. Calorim.*, **62**, 177 (2000).